IJIE

http://penerbit.uthm.edu.my/ojs/index.php/ijie
ISSN : 2229-838X e-ISSN : 2600-7916

The International Journal of Integrated Engineering

Design of Normal Mode Helical Antenna for Seawater Application

Siti Harliza Mohd Razali[1*], Razali Ngah[1], Kamilia Kamardin[2], Yoshihide Yamada[2]

[1]Wireless Communication Centre, School of Electrical Engineering, Faculty of Engineering, Universiti Teknologi Malaysia, Skudai, Johor Bahru, Johor, MALAYSIA

[2]Malaysian-Japan International Institute of Technology (MJIIT), Universiti Teknologi Malaysia, Jalan Sultan Yahya Petra, 54100 Kuala Lumpur, MALAYSIA

*Corresponding Author

DOI: https://doi.org/10.30880/ijie.2023.15.03.018
Received 7 November 2022; Accepted 29 May 2023; Available online 15 August 2023

Abstract: To overcome the substantial propagation loss in the ocean, a low frequency band should be chosen when contemplating radio wave communication. Then, the antenna used at the portable radio equipment should be very small compare to the wavelength. For the miniaturized antenna, the normal mode helical antenna (NMHA) is suitable because of achieving high efficiency. In this paper, design method of NMHA in the seawater condition (ε_r=81, σ=4) is explained. The frequency bands of 100MHz and 15MHz are selected. The self-resonant structures are determined based on the theoretical equation. Electrical characteristics such as resonant frequency, input impedance, VWSR and antenna efficiency are obtained through simulation by FEKO simulator. Electromagnetic simulation model is formed by taking into account the practical experimental condition. At 100MHz and 15MHz, resonances are ensured for antenna diameter lengths of 6.83 cm and 12.2 cm respectively. Input resistance of 27.15Ω and 94.14Ω, antenna efficiencies of -14.88dB and -26.27dB are achieved at 100MHz and 15MHz respectively.

Keywords: Small antenna, seawater, self-resonance, near-field, efficiency of NMHA

1. Introduction

Sea exploration [1], marine safety [2], monitoring underwater [3], [4], [5] an internet of underwater thing [6] technologies have recently advanced at a fast rate. The used of radio frequency (RF) wave in underwater applications, allows flexibility in the deployment of communications [7]. RF wave propagates at a velocity that is about four times faster than that of the acoustic waves in water [8]. In addition, RF waves are less sensitive to reflection and refraction in shallow waters than the acoustic waves. The multipath impact is reduced as a result of this. In designing radio link, the large propagation loss should be taken into account and low frequency bands are suitable in the seawater communication. Then the antenna should be small and have excellent performance which is NMHA. NMHA is helical antennas, a streamlined model has been suggested which model substitutes a straight-wire and inductor structure for the highly curved helix shape. The helix can be modelled with a lot fewer parts; hence analysis of the simpler model requires a lot less computing power than analysis of the whole helix [9]. The NMHA was used as a small antenna for human body application and the design equation was already developed [10].

In this paper, design method of NMHA for seawater application is clarified. First of all, rough estimation of the antenna structures is obtained by using the theoretical equation for the self-resonances [11]. Next, by using a simulation model for the practical experiment, electromagnetic simulation results such as self-resonant condition, input

*Corresponding author: author@uthm.edu.my

impedance, electric field distributions and antenna efficiency are obtained through calculation by electromagnetic simulator FEKO. The antenna efficiency is determined by the ratio of the radiation resistance to the ohmic loss resistance, and it can be clarified through the self-resonant structure. In this research, the development of a NMHA structural equation for the self-resonant condition is presented based on the electromagnetic simulation results. First, the fundamental equation of NMHA is discussed with analytical equation for NMHA, EM simulation result with self-resonance and effect of seawater model size. Next is measurement of permittivity and conductivity of seawater. Finally, the performances of the NMHA between two operational frequencies were analysed. The proposed equation is ensured through comparing the structures derived by the equation and simulations.

2. Fundamental Equation of NMHA

2.1 Analytical Equations for NMHA

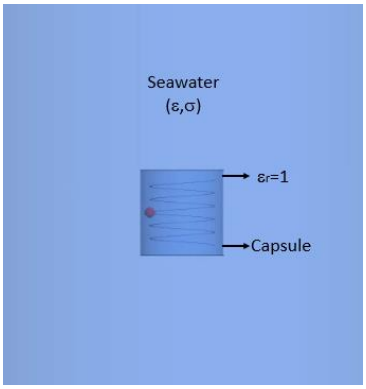

Fig. 1 - Normal Mode Helical Antenna (NMHA) in the seawater

Fig.1 show the environment of NMHA in seawater. To determine the suitable equations to develop NMHA in seawater, free space equations is referred. Usually free space is the medium to determine the suitable size of an antenna [10]. But in this paper, the equivalent equation is determined to find suitable size for NMHA in seawater. In NMHA, a helix current is separated into a straightforward current and a ring current, equivalent to an electric current source of a small dipole and a magnetic current source of a small loop. $R_D - jX_D$ and $R_L + jX_L$ are the input impedance of small dipole and small loop antennas correspondingly. R_D and R_L are the radiation resistance of the antenna, with R_D being the resistance of the small dipole and R_L being the resistance of the small loops, and specify the intemperate resistance of the antenna wire.

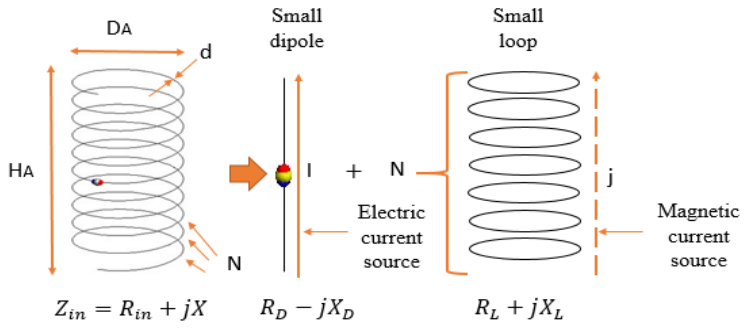

Fig. 2 - Theoretic equivalence of a normal mode helical antenna [11]

In Fig.2, the antenna length, H_A antenna diameter, D_A and number of turns N, respectively indicates the diameter of the antenna wire. NMHA can accomplish the self-resonance by selecting the sizes of H_A, D_A, and N prudently. The electrical parameters of NMHA need to be calculated for designing and fabricating process.

$$Z_{in} = R_D + R_L + R_I + j(X_L - X_D) + R_\sigma \quad (1)$$

Equation (1) shows an expression of the antenna input impedance. The self-resonant condition of NMHA is expressed by X_L=X_D, where X_L is inductive reactance and X_D is the capacitive reactance of the loop antenna and the dipole antenna. The expression of input impedance will be as the following;

$$Z_{in} = R_D + R_L + R_I + R_\sigma \tag{2}$$

2.2 EM Simulation Results for Self-Resonance

$$\sqrt{\frac{1}{\varepsilon_r}}\left(\frac{600\pi \times 19.7N\left(\frac{D}{\lambda_g}\right)^2}{9\frac{D}{\lambda_g}+20\frac{H}{\lambda_g}}\right) = \sqrt{\varepsilon_r}\left(\frac{125\frac{H}{\lambda_g}}{\pi N\left(1.1\frac{H}{\lambda_g}+\frac{D}{\lambda_g}\right)^2}\right) \tag{3}$$

Before designing the NMHA in EM software, the size is determined by deterministic equation as Equation (3). By resolving it, the self-resonant structures of an NMHA in the seawater are resolute. In Fig. 3 shows the simulation model that use for input impedance in Fig.4 and produce the graph of contrast between the equation results and the simulation results are shown in Fig. 5. Thus the parameter is stated in Table 1.

Fig. 5 shows self-resonance measured between 100MHz using N=5, and 15MHz using N=20. Permittivity is set as 81 for seawater environment and conductivity is 0. The values between calculation and simulation should be agreed well with each other. But if the conductivity become bigger the diameter size should be slightly increased. To get optimum value the seawater medium size was set half λg for every side of the antenna capsule. If the size of medium is less than that, the optimum diameter size of NMHA could not achieve self-resonance well and will become harmonic. For 100MHz, the equation value of 0.05 was not included because the value is negative, which is not a reliable value for this case N=5. From analysis of capsule gap of NMHA, the diameter of NMHA become large if the size of capsule gap increased. The equation (3) is such an ideal size usually with capsule gap 1mm. But for real experimental circumstance the gap is more than 1mm. That's why the graph from Fig. 5 is differ slightly bigger from the Equation (3) line for 100MHz. But for 15MHz the equation (3) and simulation is agreeing well for each other.

Simulating NMHA with FEKO EM also revealed the input impedance that is suitable for the antenna. From the simulation, the input impedance showed that impedance matching is good when the value of Zin is 0. The values in the Smith chart and the operational frequency chosen are read and this happened when the Zin is about 0Ω to 94Ω when the antenna is in seawater with conductivity that equaled to 0,1 and 4. To build a better NMHA, the structure of port changed to tap port to improve the mismatch loss [12]. Fig. 4 shows the pattern of input impedance for different frequencies at different conductivities. It shows higher conductivity as the shape of input impedance is closed to matching impedance.

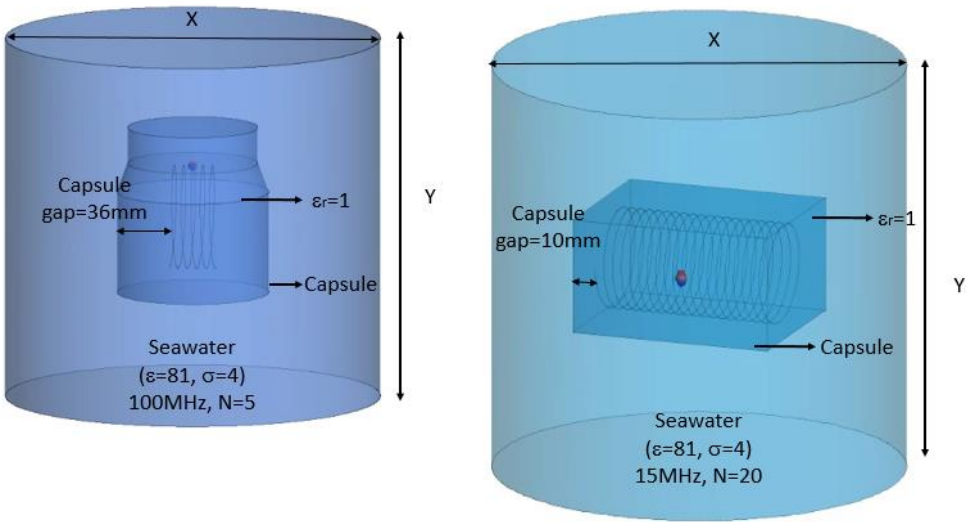

Fig. 3 - Simulation model for experimental setup for 100MHz using 5 turns and 15MHz using 20 turns

Table 1 - Parameter of simulation model at 0.1 H/λ

Aspect	**Parameter**		
Simulator	**Altair FEKO 2019**	**Method of Moment**	
Frequency	VHF	100 MHz	15 MHz
	Wavelength, λ_0	3 m	20 m
Seawater	Wavelength, λ_g	33.3 cm	222.2 cm
	Permittivity, ε_r	81 F/m	81 F/m
	Conductivity, σ	0, 1 and 4 S/m	0, 1 and 4 S/m
	Mass density, ρ	1000 kg/m^3	1000 kg/m^3
	Mesh size, Δm	λ/25 (Fine)	λ/25 (Fine)
NMHA	Material	Copper	Copper
	Conductivity, σ	58 x 10^6 [1/Ωm]	58 x 10^6 [1/Ωm]
	Height, H/λg	0.1, H=3.3cm	0.1, H=22.2cm
	Diameter, D/λg	0.1915, σ=0, D=6.32cm 0.2036, σ=1, D=6.72cm 0.20697, σ=4, D=6.83cm	0.053829, σ=0, D=11.95cm 0.054955, σ=1, D=11.98cm 0.053964, σ=4, D=12.2cm
	Diameter of wire, d (cm)	0.2	0.2
	Number of turns, N	5	20
	Mesh size, Δl	λ/25 (Fine)	λ/25 (Fine)

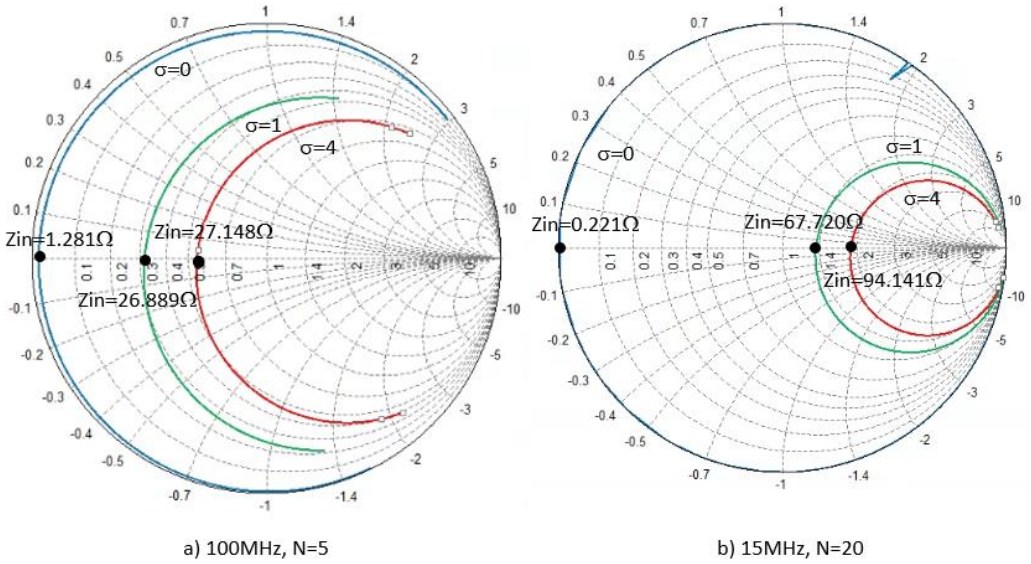

Fig. 4 - Input impedance values for 100MHz and 15MHz operating frequencies with different conductivities

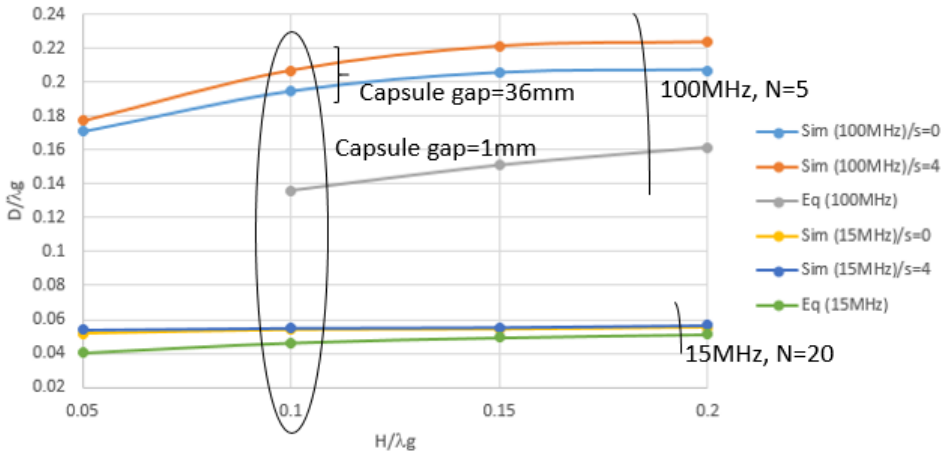

Fig. 5 - Simulated and calculated self-resonance at frequencies of 15MHz and 100MHz

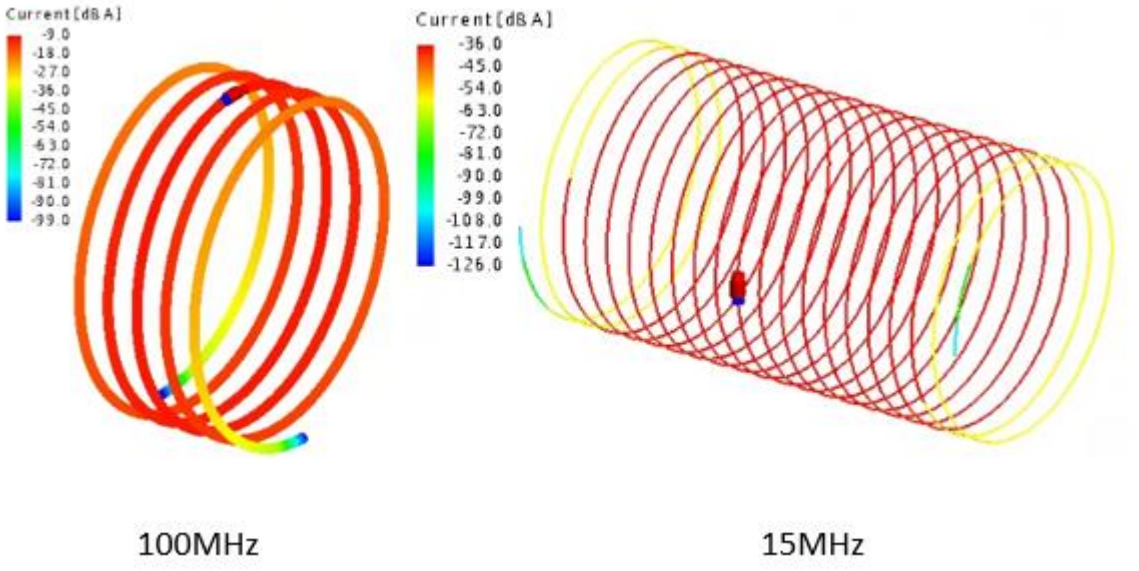

Fig. 6 - Current distribution of NMHA at 100MHz and 15MHz

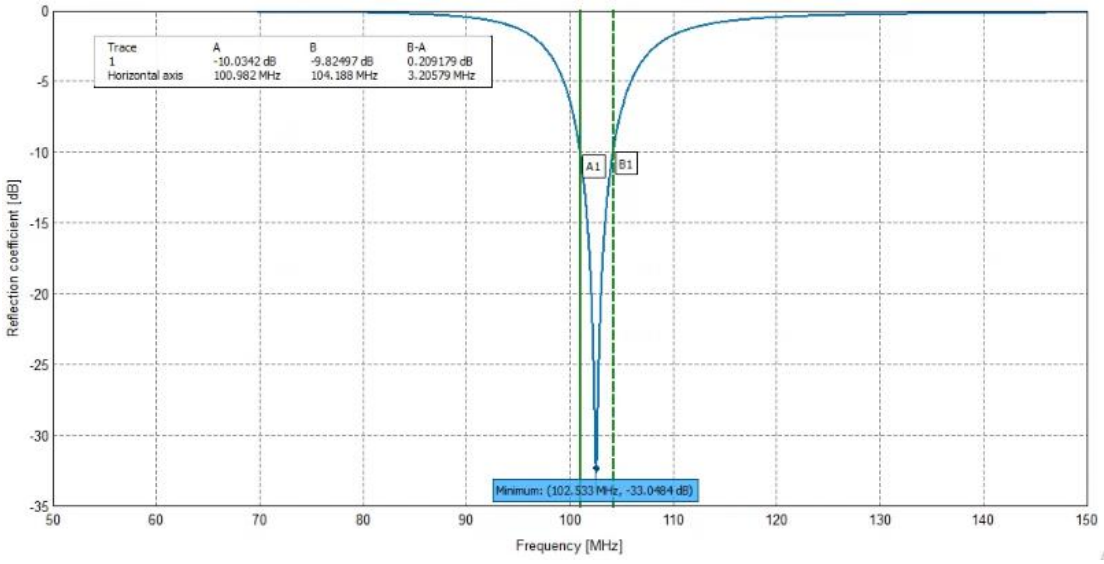

Fig. 7 - S11 and bandwidth of NMHA at 100MHz

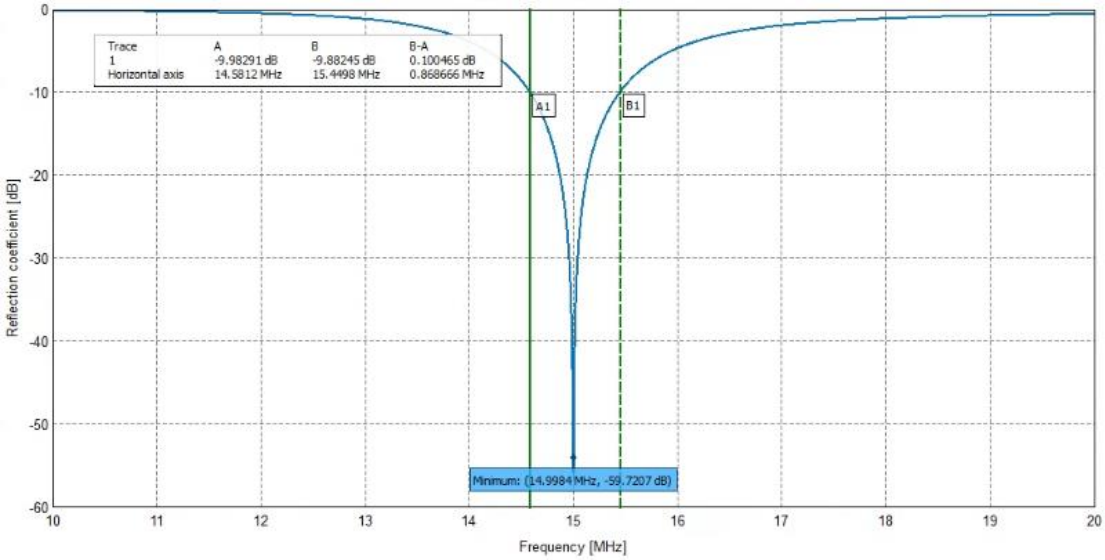

Fig. 8 - S11 and bandwidth of NMHA at 15MHz

Firstly, the expected size is determined from Fig. 5 and the suitable size was chosen at one point from H/λ_g when developing the NMHA in seawater medium by FEKO EM. Then, the model with the estimated size of NMHA is designed in FEKO EM to measure its performances. Fig. 3 shows the simulation model that was used in the simulation, and the dimensions of each part of the NMHA where the antennas were put into free space capsules before they are put in the seawater medium to avoid short circuit. The models had N turns and one power port in the middle of the ring. It also shows that the differences between the two operating frequencies in terms of sizes and turns. The operating frequency is different, making the sizes and turns different. Theoretically, the lower the frequency, the greater the size of antenna. Because NMHA is a type of small antenna, the lower frequency can make the antenna smaller than the other types of antennas, such as patch or micro strip antenna of the same operating frequencies. Table 1 shows some parameters that are used in this simulation with the NMHA exact size and the performances of that antenna investigated. There are several parameters that differed to make the NMHA a good antenna for the operation frequencies that is chosen.

Fig. 6, shows that the current distribution of NMHA for 15MHz is higher than 100MHz, where the red colour presenting the strong current area is greater. Approximately at H/2, the extreme current (Imax) is perceived at the center of the wire (red colored area). The current distribution is narrowing towards the end of the antenna, where the minimum current (Imin) is in dark blue. A strong current area for 15MHz is concentrated more at the center of the antenna compared to 100MHz antenna because it has more turns than 100MHz.

Fig.7 and Fig.8 shows the S11 value and bandwidth value for the both frequencies. There are 102.5MHz at -33dB and 3.21MHz for 100MHz, 14.998MHz at -59.72dB and 0.87MHz for 15MHz. Both shows frequencies have a lot of transmitted power from the antenna because the value of S11 is lower than -20dB.

2.3 Effect of Seawater Model Size

The environment situation between simulation and real is explored when designing seawater antenna. This part purposed is to determine laboratory experimental structure of the NMHA. Fig.6 shows the model of simulation setup for experimental condition. The result from that simulation is analyzed by the surface current and current are using 3 sizes of seawater medium. There is size 1, size 2 and size 3 which shows the surface current is become less from size 1 to size 3 in Fig.8 and Fig.9. But the input impedance of these three sizes are same value. The details of sizes are stated in Table 2. This indicates that the volume of seawater does not change the size of NMHA. Therefore, the size of the seawater container can be used accordingly to what is available in the experimental lab. Furthermore, performance of these two NMHA are analyzed and it shows that the antenna efficiency (η) of 15MHz was higher than 100MHz. By using Equation (4), antenna efficiency (η) can be obtained. To determined efficiency, the (Ra) resistance value is obtained by setting the wire conductivity (σ=∞) to a very large value such as 10^{15} S/m. Because equation (5), R_l becomes 0 as the σ becomes infinity. Table 2 shows the value of R_{in}, R_a and antenna efficiency. Consequently, the resistance for different conductivity is shown in Fig. 4. The value of efficiency in dB lessened as the value of conductivity increased.

$$\eta = \frac{R_a}{R_{in}} \tag{4}$$

$$R_{in}(\sigma) = R_a + R_l \tag{5}$$

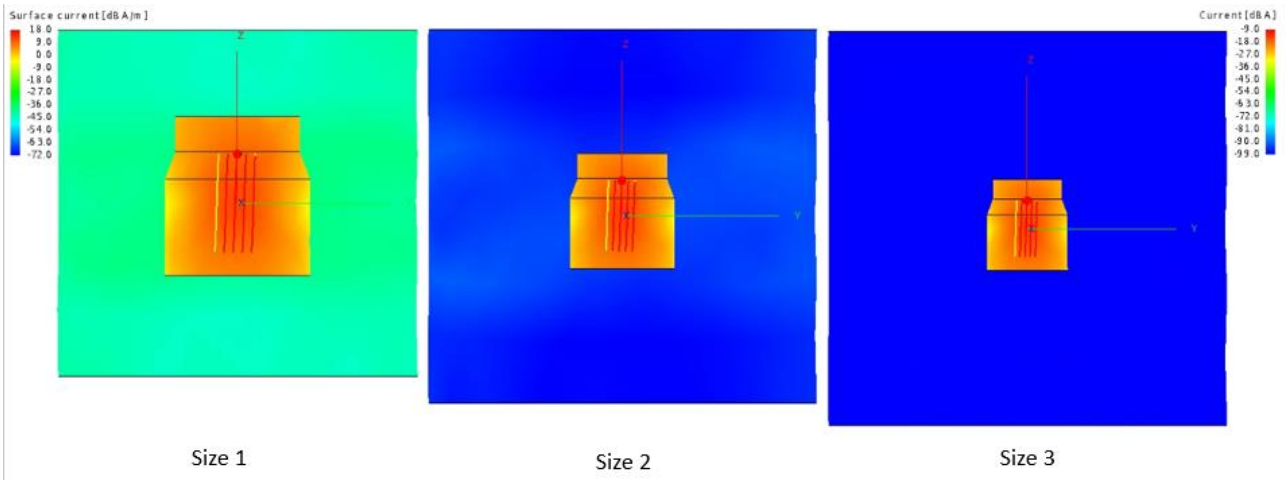

Fig. 8 - Surface current and current value between 3 sizes for 100MHz

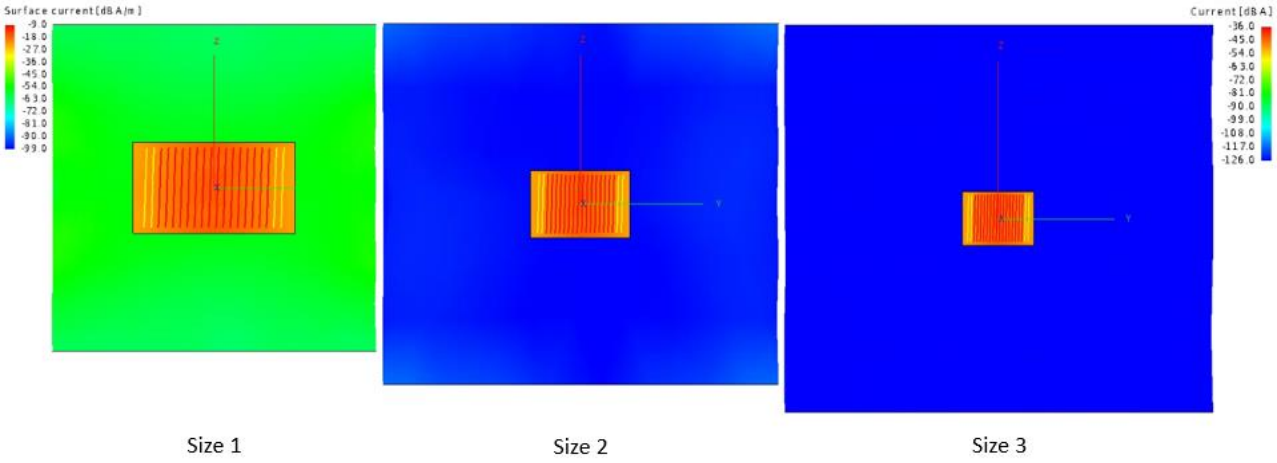

Fig. 9 - Surface current and current value between 3 sizes for 15MHz

Table 2 - Data for effect of seawater model size

Frequency (MHz)	Parameter	Size 1	Size 2	Size 3
100	Size Dimension (cm)	X=26, Y=25	X=36, Y=30	X=39, Y=37.5
	Input impedance, Rin (Ω)	31.242	31.249	31.311
	Ra (Ω)	1.015	0.994	5.861
	Efficiency (η dB) (10 log Ra/Rin)	-14.88	-14.97	-7.28
15	Size Dimension (cm)	X=50, Y=50	X=100, Y=75	X=150, Y=100
	Input impedance, Rin (Ω)	94.147	94.894	94.883
	Ra (Ω)	0.222	0.186	0.064
	Efficiency (η dB) (10 log Ra/Rin)	-26.27	-27.08	-31.71

3. Measurement of Seawater Permittivity and Conductivity

Conductivity of seawater is a significant indicator of oceanic electromagnetic properties. Thus directly effects the electromagnetic attenuation characteristics and phase distribution structures of the ocean. Previous works have considered how the combined effects of salinity, temperature and pressure are affects the vertical conductivity distribution and its formation mechanisms. Few studies have examined how salinity, temperature, and pressure interact to impact the vertical conductivity distribution and the processes that lead to it in [13]. There are several methods to determine the value of conductivity of seawater. In [14] offers a dual-coil method for measuring the conductivity of seawater via magnetic resonance coupling. While [15], a three-layer wavelet neural network with seven hidden nodes serves as the prediction model and [16] is the fresh model (dielectric constant as a function of salinity, temperature, and frequency) uses the functional form for conductivity, σ (S, T), that is provided by the definition of salinity and fits the same measurement as reported in earlier work. It is based on the response of a polar molecule proposed by Debye. Method to measure the dielectric of seawater in this research by using coaxial probe method and vector network analyzer as Fig.10. In the result's screen, ε' and ε'' are the main result that take and calculated to get tangent delta and conductivity. The value of ε' is permittivity value and conductivity value is calculated using equation (6) to (11).

$$\varepsilon = \varepsilon_r + j\varepsilon_i \tag{6}$$

$$\varepsilon_r = \varepsilon^{'}\varepsilon_0 \tag{7}$$

$$\varepsilon_i = \varepsilon^{''}\varepsilon_0 \tag{8}$$

$$\sigma = \omega\varepsilon^{'}\varepsilon^{''}\tan\delta \tag{9}$$

$$\tan\delta = \frac{\varepsilon^{''}}{\varepsilon^{'}} \tag{10}$$

$$\omega = 2\pi f \tag{11}$$

In measuring the conductivity of seawater, readings are taken as many as 15 samples at a frequency of 100 MHz by using artificial seawater and pure seawater that are taken in the area near the Telok Nipah Jetty, Pulau Indah Port Klang. The readings have been averaged and the values are close to the values used by previous research. The values are as shown in Table 3.

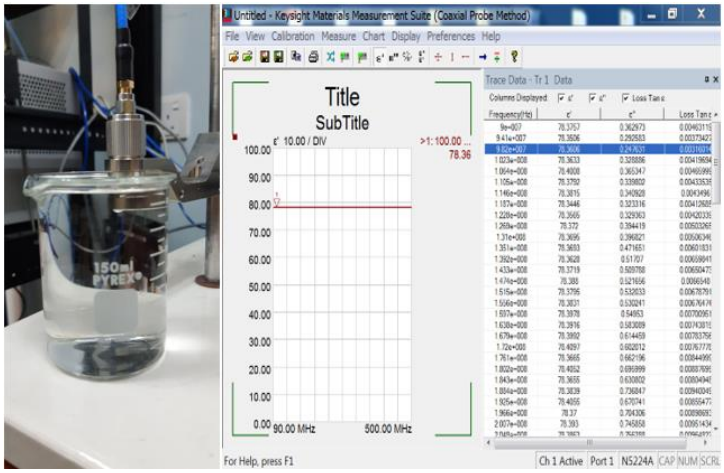

Fig. 10 - Seawater permittivity and conductivity measurement

Table 3 - Permittivity and conductivity of seawater

Type of Seawater	Permittivity (ε)	Conductivity (σ)
Artificial seawater	82.68	3.45
Pure seawater	84.44	4.08
Theory value	81	4

4. Conclusion

From the antenna performances, both antennas gave the best performance for their respective frequencies. As lower frequency has long lambda, the NMHA with 15MHz had better performance than 100MHz because its efficiency was higher than 100MHz. But both frequencies can be used in seawater. All that is needed is to just choose the frequency according to the application suitable for it. For future works, the sample will be measured using seawater taken from the jetty at Telok Nipah, Pulau Indah, Port Klang. This paper contributes to the NMHA antenna application in seawater, as previous works has already shown the NMHA application in medical sensor.

Acknowledgement

The authors would like to thank the Ministry of Higher Education (MOHE), Jabatan Pengajian Politeknik dan Kolej Komuniti (JPPKK), Wireless Communication Centre (WCC), School of Postgraduate Studies (SPS), Research Management Centre, Communication Systems and Network (CSN i-Kohza) Research Group, Malaysia - Japan International Institute of Technology (MJIIT) and Universiti Teknologi Malaysia (UTM) for the support of the research.

References

[1] J. Chen, Y. Xin, Y. Zhang, J. Li, W. Yang, and Z. Li, "A Novel Deep-sea Exploration Equipment : Combined Multisite Lander and Rover ROV System," pp. 2-6, 2021.
[2] K. Bao, D. Shang, R. Wang, and R. Ma, "AIS big data framework for maritime safety supervision," *Proc. - 2020 Int. Conf. Robot. Intell. Syst. ICRIS 2020*, no. 2012, pp. 150-153, 2020.
[3] A. Danisor and R. Constantinescu, "Monitoring Beacons," 2022.
[4] A. Dala and T. Arslan, "Design, implementation, and measurement procedure of underwater and water surface antenna for lora communication," *Sensors (Switzerland)*, vol. 21, no. 4, pp. 1-18, 2021.
[5] K. M. Alaaudeen and A. I. Rayhana, "A CONFORMABLE DESIGN OF A Conformable Design of Hemispherical Helical Antenna for HELICAL Ocean Monitoring HEMISPHERICAL ANTENNA FOR OCEAN MONITORING," no. March, pp. 49-53, 2019.
[6] Z. A. H. Qasem, H. Esmaiel, H. Sun, J. Wang, Y. Miao, and S. Anwar, "Enhanced fully generalized spatial modulation for the internet of underwater things," *Sensors (Switzerland)*, vol. 19, no. 7, pp. 1-16, 2019.
[7] G. S. Spagnolo, L. Cozzella, and F. Leccese, "Underwater optical wireless communications: Overview," *Sensors (Switzerland)*, vol. 20, no. 8, 2020.
[8] O. Aboderin, "Antenna Design for Underwater Applications," 2019.
[9] C. Su, H. Ke, and T. Hubing, "Corrections to 'A simplified model for normal mode helical antennas,'" *Appl.*

Comput. Electromagn. Soc. J., vol. 25, no. 8, p. 722, 2010.
[10] D. T. Dung, Q. D. Nguyen, D. Q. Trinh, and Y. Yamada, "Investigating equations used to design a very small normal-mode helical antenna in free space," *Int. J. Antennas Propag.*, vol. 2018, 2018.
[11] N. T. Tuan *et al.*, "Deterministic equation of self-resonant structures for normal-mode helical antennas implanted in a human body," *IEEE Antennas Wirel. Propag. Lett.*, vol. 17, no. 8, pp. 1377-1381, 2018.
[12] N. Q. Dinh, N. Michishita, Y. Yamada, and K. Nakatani, "Design method of a tap feed for a very small normal-mode helical antenna," *APMC 2009 - Asia Pacific Microw. Conf. 2009*, pp. 2416-2419, 2009.
[13] Z. Zheng, Y. Fu, K. Liu, R. Xiao, X. Wang, and H. Shi, "Three-stage vertical distribution of seawater conductivity," *Sci. Rep.*, vol. 8, no. 1, pp. 1-10, 2018.
[14] N. Liu, Y. Miao, T. Wang, Y. Wu, and J. Zhao, "A Seawater Conductivity," *IEEE Instrum. Meas. Mag.*, vol. 26, no. February, pp. 58-65, 2023.
[15] F. Qin, Z. Pan, W. Li, H. Wang, and M. Q. H. Meng, "A wavelet neural network based prediction for conductivity of seawater," *2018 IEEE Int. Conf. Inf. Autom. ICIA 2018*, no. August, pp. 893-896, 2018.
[16] D. M. Le Vine, Y. Zhou, and R. H. Lang, "Model for Dielectric Constant of Seawater Based on L-Band Measurements With Conductivity by Definition," *IEEE Geosci. Remote Sens. Lett.*, vol. 19, pp. 1-5, 2022.